Determination of streamer depth and sensor calibration from dual-sensor streamer data

Anthony Day, Endrias Asgedom, Neil Turnbull, PGS.*

Summary

Dual-sensor streamer acquisition allows the incident wavefield to be decomposed into up- and down-going parts. This operation can be performed for any arbitrary recording surface, and the data can subsequently be redatumed to emulate any desired acquisition geometry. In order to take advantage of this flexibility, it is necessary that the streamer profile is accurately known. In this paper, we demonstrate that dual-sensor streamer data can be used to derive the streamer depth profile. This is achieved by cross-ghosting, whereby the pressure data are convolved with the particle velocity ghost and vice versa such that they should be identical. The optimum apparent depth that minimizes the residual error in the cross-ghosted data can be derived for each shot and channel independently. This apparent depth shows the imprint of the rough sea surface, which can be eliminated by averaging the results for many shots. This procedure provides an independent verification of the information obtained from the depth sensors in the streamer, which can be used to identify calibration problems such that they can then be rectified whilst the survey is ongoing. After finding the optimal depth, the remaining residual error can be used to determine residual errors in the sensor calibration. These errors are shown to be very small.

Introduction

A dual-sensor streamer records the pressure and vertical component of particle velocity using collocated sensors. These data permit the decomposition of the wavefield into up- and down-going parts, which can optionally be redatumed to any output datum level (Carlson et al., 2007). The theoretical basis of the wavefield decomposition method is the field reciprocity theorem. Fokkema and van den Berg (1993) showed how wavefield decomposition can be performed for any continuous recording surface given measurements of pressure and the particle velocity normal to the recording surface. Söllner et al. (2008) demonstrated a practical application of this theory to dual-sensor streamer field data.

These features of dual-sensor streamer data permit great flexibility in acquisition design. Streamers can be towed with whatever depth profile is most convenient from an operational or geophysical perspective, and the ability to perform wavefield decomposition and independent redatuming of the up- and down-going wavefields allows any other streamer profile to be emulated. This was demonstrated by means of a time-lapse experiment described by Day et al. (2010). They showed that dual-sensor streamer data acquired at 15m depth could be used to match conventional streamer data acquired at 8m depth with a repeatability that is consistent with that achievable for conventional time-lapse acquisition where the streamer depths are repeated. Furthermore, since there is no theoretical restriction on the streamer profile, there is no reason that a horizontal profile must be chosen. Lesnes et al. (2014) demonstrated the use of a slanted dual-sensor streamer profile to permit the streamer to be towed at an increased average depth, with consequent signal-to-noise ratio benefits, whilst negating the operational difficulties associated with applying the downward force to the fronts of the streamers necessary to attain depths in excess of 20m.

A necessary prerequisite to take advantage of the flexibility in acquisition design outlined above is that the streamer profile is known. The wavefield decomposition itself is substantially insensitive to streamer depth variations since, for all practical geometries of interest, the streamer profile is locally very close to horizontal. However, any subsequent redatuming operations require accurate knowledge of the depth of the sensors. This streamer depth is obtained from hydrostatic pressure sensors located within the streamers. In this paper, we demonstrate how the dual-sensor streamer data itself can be used to obtain an independent measure of the streamer depth. This can be used to validate the information obtained from the depth sensors and provides additional confidence that the streamer profiles are well known.

A further issue related to processing dual-sensor streamer data is that the pressure and particle velocity data are recorded by different instruments with different responses that must be matched prior to wavefield decomposition. We show that this sensor matching can also be calibrated using the dual-sensor streamer data.

Method

The basis for deriving streamer depth and sensor calibration information from dual-sensor streamer data is the concept of cross-ghosting. The sea surface ghost manifests differently on the pressure and particle velocity data. The sea surface has a reflection coefficient approximately equal to -1, and the omnidirectional pressure sensor records this polarity reversal such that the ghost has opposite polarity to the corresponding primary. For the vertical particle velocity, this polarity reversal is counteracted by the directionality of the sensor with the result that the ghost has the same polarity as the primary. Cross-ghosting involves convolution of the pressure data with an assumed particle

DOI http://dx.doi.org/10.1190/segam2014-1067.1

velocity ghost function and vice versa. After cross-ghosting, the two datasets should be identical and have twice the ghost period of the input data. This behavior is illustrated schematically in Figure 1.

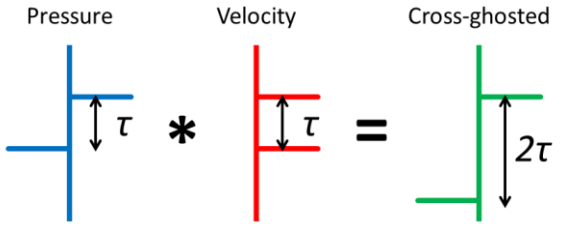

Figure 1: Ghost functions for pressure and particle velocity data and the ideal cross-ghosting result.

A practical application of cross-ghosting must take account of the variation in ghost period with emergence angle, an obliquity scaling to account for the amplitude difference at non-zero emergence angle between the omnidirectional pressure sensor and a particle motion sensor that is oriented normal to the recording surface, and the acoustic impedance scalar that relates pressure and velocity. For a horizontal streamer, the cross-ghosting equations can be expressed in the frequency-wavenumber domain as follows:

$$P_{xg}(\omega, k_x) = \frac{k_z}{\omega\rho}\left(1 + e^{-2ik_z z}\right)P(\omega, k_x)$$
$$V_{xg}(\omega, k_x) = \left(1 - e^{-2ik_z z}\right)V(\omega, k_x)$$

P and V are pressure and vertical particle velocity respectively, the suffix xg indicates cross-ghosting, ρ is density, z is the receiver depth, ω and k_x are the angular frequency and horizontal inline wavenumber respectively, and k_z is the angular vertical wavenumber expressed as:

$$k_z = \sqrt{(\omega/v_w)^2 - {k_x}^2}$$

where v_w is the speed of sound in water.

The equations above require that the streamer depth is known. Furthermore, it is implicitly assumed that the responses of the pressure and particle velocity sensor have been matched prior to the application of cross-ghosting. If either of these assumptions is incorrect, the cross-ghosted pressure and particle velocity will not be identical. We seek the optimum depth and sensor calibration filters that minimize the difference between cross-ghosted pressure and particle velocity. A similar method was applied to ocean bottom cable data by Soubaras (1996). Note that the equations are strictly correct only for horizontal streamers and the ghost model assumes a reflection coefficient of -1. Both of these assumptions are reasonable for the streamer geometries (locally close to horizontal) and bandwidth under consideration under realistic acquisition conditions. However, neither assumption represents a fundamental theoretical limitation of the method, which could be generalized to any streamer profile and sea surface behavior if required.

The effects of depth and sensor calibration errors can be distinguished by considering how they affect the residual error when cross-ghosted particle velocity data is subtracted from cross-ghosted pressure data. These effects are illustrated by the schematic in Figure 2. A depth error results in an inaccurate estimate of the ghost period ($\hat{\tau}$ in Figure 2), which gives rise to a residual error after cross-ghosting near the location of the original ghost in the recorded data. If the depth is correct but the sensor calibration is incorrect, Figure 2 illustrates that the residual error will be concentrated near the location of the primary and the ghost after cross-ghosting. This schematic provides a simple means for qualitative analysis of cross-ghosting residuals in order to ascertain their likely cause.

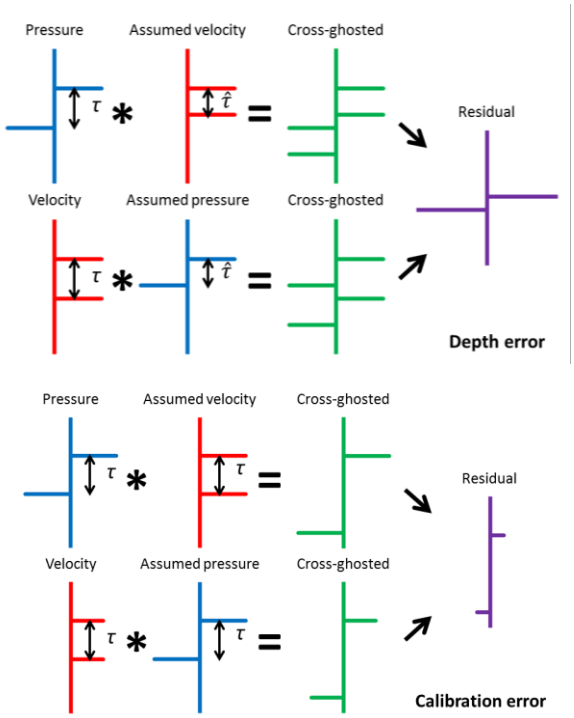

Figure 2: Effect of cross ghosting and the resulting residual errors in the presence of an error in the assumed depth (top) and sensor calibration (bottom).

DOI http://dx.doi.org/10.1190/segam2014-1067.1

Finally, note that in order to exploit this technique it is advantageous to have access to data with high signal-to-noise ratio over the broadest possible bandwidth. All subsequent analysis presented in this paper is performed for a window surrounding the seafloor reflector. A 15-20Hz low-cut filter has been applied to both pressure and particle velocity datasets, which is necessary to exclude that part of the data that is contaminated with strong mechanical noise.

Streamer depth determination

Cross-ghosting analysis was applied to data acquired using a streamer profile with a nominal depth of 15m at channel 1 increasing linearly to a maximum depth of 30m at channel 350, with constant 30m depth at all higher channel numbers. This dataset was chosen in order to demonstrate that the method is applicable to general streamer profiles and is not reliant on a substantially invariant cable depth.

Figure 3 shows the results of cross-ghosting in a window centered on the seafloor reflector for a single shot gather. After cross-ghosting the pressure and particle velocity data should be very similar, and Figure 3 demonstrates that this is the case. Inspection of the residual error shows that most of the energy is located between the primary and the ghost location after cross-ghosting. Comparison with Figure 2 indicates that the major contributing factor to this residual is likely to be an error in the estimated ghost period arising from the use of an incorrect depth. The first step in the optimization is therefore to find the apparent depth that minimizes the residual error after cross-ghosting for each channel independently. Figure 3 demonstrates that the optimal result has substantially reduced this residual error.

Figure 4 compares the streamer depth profile obtained from the depth sensors and the apparent depth obtained using cross-ghosting analysis. The two depth profiles follow the same general trend, which indicates that the two measures are broadly consistent with each other. However, there is

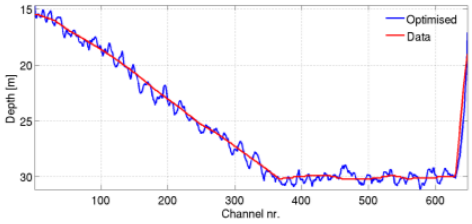

Figure 4: Streamer profile for a single shot derived from the depth sensors (red) and cross-ghosting analysis (blue).

much more local variation around the general trend in the depths obtained from cross-ghosting analysis. Furthermore, this variation is not random: groups of adjacent channels give results that are systematically either deeper or shallower than the general trend. These discrepancies reflect the effect of the rough sea surface. Apparent depths obtained from cross-ghosting reflect the distance between the receiver location and a local average of the sea surface for arrivals within the analysis window. The deviations from the general trend are of similar magnitude to those obtained using more sophisticated sea surface imaging techniques (Orji et al., 2010).

In order to identify discrepancies between the streamer depths recorded by the depth sensors and those obtained from cross-ghosting analysis, it is necessary to eliminate local sea surface effects by averaging the results for many shots. Figure 5 shows the results of such analysis applied to data acquired using a streamer with a nominally horizontal profile. Two prominent anomalies are visible where the average streamer depth derived from the data differs significantly from the neighboring locations even though the data from the depth sensors suggested that the streamer was close to horizontal. Subsequent in-sea calibration of the depth controllers nearest the location of these anomalies revealed a calibration error of the order of 0.6m, which is similar to that indicated by the cross-ghosting analysis.

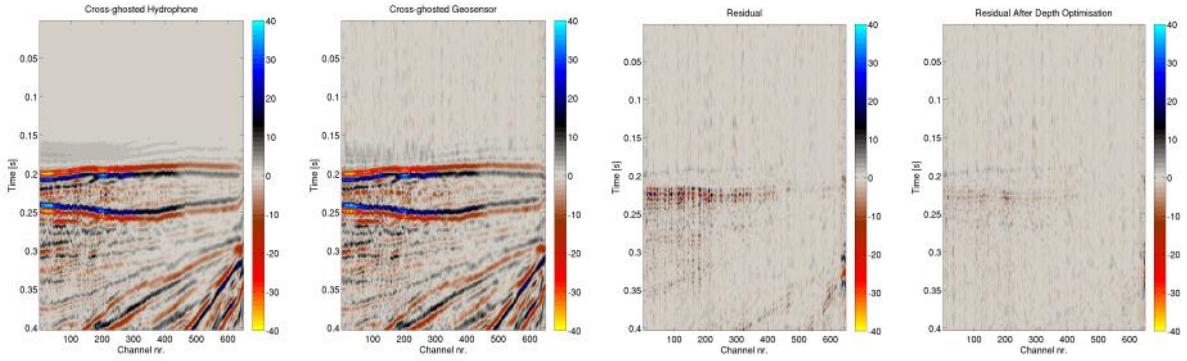

Figure 3: Cross ghosting analysis for one shot gather. A static shift has been applied to flatten the seafloor reflector for display purposes.

DOI http://dx.doi.org/10.1190/segam2014-1067.1

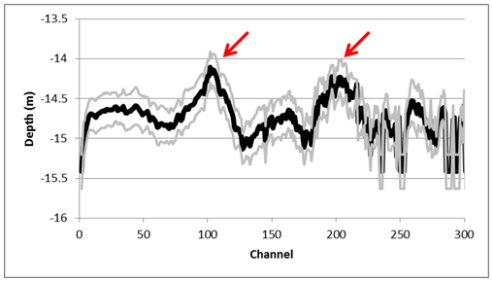

Figure 5: Mean streamer profile for 200 shots derived from cross-ghosting, plus the one standard deviation error bar (grey). The nominal streamer profile should be horizontal – note the deviations near channels 102 and 198 (red arrows). These are related to malfunctioning depth sensors.

This example illustrates how cross-ghosting analysis can be used as a near-real-time quality control tool to validate the data provided by the depth sensors and take remedial action if discrepancies are identified.

Sensor calibration

Before combining the pressure and particle velocity data, the two datasets must be matched. In general this is a much simpler task for towed streamer acquisition compared to receivers located on the ocean bottom because the properties of water that relate pressure and particle velocity (density and propagation velocity) can be measured and tend to vary smoothly in space. The medium properties can thus be accounted for robustly, so the only remaining factor that needs to be taken into account is the relative responses of the particle velocity and pressure sensors, which are known. Consequently, there is no need to invoke any statistical matching as commonly has to be applied to ocean bottom sensors, with all the attendant uncertainty: for dual-sensor streamer data, sensor matching is a fully deterministic process.

Figure 3 shows that, after optimizing for the apparent sensor depth, the remaining residual errors are very small for all channels. This indicates that the sensor matching has been successful. Nevertheless, we can seek to minimize the residual error still further by assuming that any remaining residual relates to inaccurate sensor matching. Since the sensor responses are invariant, a single correction is derived for each channel that minimizes the remaining residual for all shots. Figure 6 shows the result for a single channel in the frequency domain. This result further confirms that the original sensor calibration is very accurate: the residual sensor calibration leads to only very minor changes. That such small deviations can be detected serves to illustrate that cross-ghosting analysis is a highly sensitive tool that can provide independent quality control of the sensor calibration information.

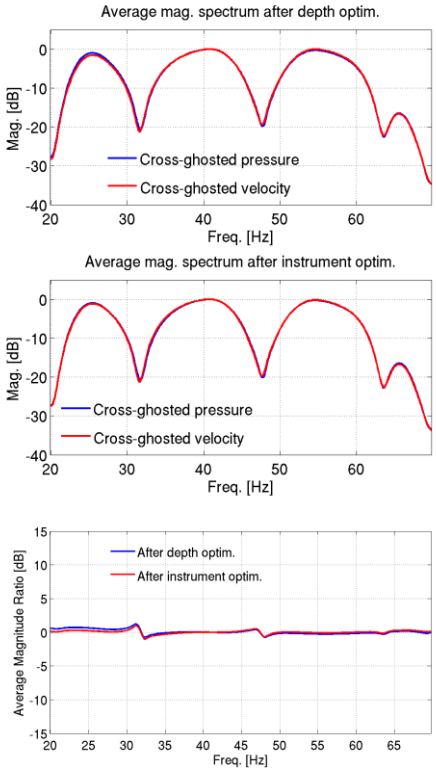

Figure 6: Mean cross-ghosted pressure and particle velocity spectra for channel 300 from the data shown in Figure 3 after depth optimisation (top), and after additional residual sensor calibration (middle). The amplitude ratio between cross-ghosted pressure and particle velocity is also shown (bottom).

Conclusions

A dual-sensor streamer permits the decomposition of the wavefield into up- and down-going parts for any arbitrary recording surface. This requires that the depth of the streamers is known and that the two sensors have been properly matched. Cross-ghosting analysis, whereby the pressure data are convolved with the particle velocity ghost and vice-versa, can be used to independently verify the accuracy of these depths and calibration. After cross-ghosting, the pressure and particle velocity data should be identical. Apparent depth and sensor matching filters can be found that minimize the residual error. This procedure can be used as a quality control tool in near-real-time. In particular, unreliable depth sensors that would otherwise go undetected can be identified and recalibrated in the field.

Acknowledgments

We thank the crews of Ramform Viking and Ramform Challenger who acquired the data presented in this paper, and PGS for permission to publish the results.

DOI http://dx.doi.org/10.1190/segam2014-1067.1

http://dx.doi.org/10.1190/segam2014-1067.1

EDITED REFERENCES

Note: This reference list is a copy-edited version of the reference list submitted by the author. Reference lists for the 2014 SEG Technical Program Expanded Abstracts have been copy edited so that references provided with the online metadata for each paper will achieve a high degree of linking to cited sources that appear on the Web.

REFERENCES

Carlson, D., A. Long, W. Söllner, H. Tabti, R. Tenghamn, and N. Lunde, 2007, Increased resolution and penetration from a towed dual-sensor streamer: First Break, **25**, no. 12, 71–77.

Day, A., M. Widmaier, T. Høy, and B. Osnes, 2010, Time-lapse acquisition with a dual-sensor streamer over a conventional baseline survey: First Break, **28**, no. 12, 79–87.

Fokkema, J. T., and P. M. van den Berg, 1993, Seismic applications of acoustic reciprocity: Elsevier Science Publishing.

Lesnes, M., A. Day, and M. Widmaier, 2014, Increased streamer depth for dual-sensor acquisition — Challenges and solutions: Presented at the 76th Annual International Conference and Exhibition, EAGE.

Orji, O., W. Söllner, and L. J. Gelius, 2010, Imaging the sea surface using a dual-sensor towed streamer: Geophysics, **75**, no. 6, V111–V118, http://dx.doi.org/10.1190/1.3496439.

Söllner, W., A. Day, and H. Tabti, 2008, Space-frequency domain processing of irregular dual-sensor towed streamer data: 78th Annual International Meeting, SEG, Expanded Abstracts, 1078–1082.

Soubaras, R., 1996, Ocean bottom hydrophone and geophone processing: 66th Annual International Meeting, SEG, Expanded Abstracts, 24–27.